JPE 16-3-26

http://dx.doi.org/10.6113/JPE.2016.16.3.1087
ISSN(Print): 1598-2092 / ISSN(Online): 2093-4718

A Comparative Study of Two Diagnostic Methods Based on the Switching Voltage Pattern for IGBT Open-Circuit Faults in Voltage-Source Inverters

Yuxi Wang*, Zhan Li*, Minghui Xu*, and Hao Ma†

*,†School of Electrical Engineering, Zhejiang University, Hangzhou, China

Abstract

This paper reports an investigation conducted on two diagnostic methods based on the switching voltage pattern of IGBT open-circuit faults in voltage-source inverters (VSIs). One method was based on the bridge arm pole voltage, and the other was based on bridge arm line voltage. With an additional simple circuit, these two diagnostic methods detected and effectively identified single and multiple open-circuit faults of inverter IGBTs. A comparison of the times for the diagnosis and anti-interference features between these two methods is presented. The diagnostic time of both methods was less than 280ns in the best case. The diagnostic time for the method based on the bridge arm pole voltage was less than that of the method based on the bridge arm line voltage and was 1/2 of the fundamental period in the worst case. An experimental study was carried out to show the effectiveness of and the differences between these two methods.

Key words: Bridge arm line voltage, Bridge arm pole voltage, Fault diagnosis, Open-circuit faults, Voltage-source inverter

I. INTRODUCTION

Voltage source inverters (VSIs) are widely used in variable speed electric motor drives, uninterrupted power systems, active power filters, and more recently, in renewable energy conversion systems and electric vehicles. An accident due to faults in VSIs can result in severe damage to human life and environments especially in applications such as aerospace, medical and military. Thus, the reliability of VSIs is an important factor in ensuring their safe, continuous and high performance operation under different types of faults. Therefore, the development of fault diagnostic methods has generated a great deal of research interest during the past few years [1]-[6].

Most of the components in power circuits age and even become damaged during operation. A number of published reports [1], [2] on the faults in power electronics have established the proportion of various types of faults in terms of the total failures: capacitor faults 30%, printed circuit board (PCB) faults 26%, semiconductor faults 21%, solder faults 13% and connector faults 3%. According to a survey of 56 enterprises, semiconductor power devices were selected as most fragile by 31% of the responders [3].

Many publications [4]-[6] are available on capacitor fault detection and identification. IGBTs were found to be an appropriate choice in VSIs because of their high efficiency, fast switching and high power application features. However, their high probability of failure in the switching devices exists due to their high electrical and thermal stresses [7]-[9]. In general, the power transistor failures in VSIs can be broadly categorized into three types of faults namely, open-circuit, short-circuit and intermittent gate-misfiring faults. Although an IGBT can handle short-circuit currents for 10μs, overcurrent or short-circuit protection is a standard feature provided in industrial products. The rapid detection of short-circuit faults is a challenge and needs additional research. The intermittent gate-misfiring fault is an early manifestation and turns into an open-circuit fault in many instances. A method for the on-line detection of the intermittent gate-misfiring of the switching devices in voltage-fed PWM inverters has been developed [7]. It was based on a time-domain response analysis of the current space vector of an induction motor since a frequency analysis was inapplicable.

Open-circuit faults in general are not harmful to inverters

Manuscript received Sep. 12, 2015; accepted Jan. 9, 2016
Recommended for publication by Associate Editor Kyo-Beum Lee.
†Corresponding Author: mahao@zju.edu.cn
Tel: +86-159-6714-6068, Fax: +86-571-8795-3985, Zhejiang Univ.
*School of Electrical Engineering, Zhejiang University, China

and do not cause system shutdowns. However, they can lead to secondary failures of other components resulting in total system shutdowns and high repair costs [8], [9]. The occurrence of open-circuit faults is frequent in power systems and deteriorates the system performance. A large amount of literature has attempted to address this type of failure.

Several methods have been based on the output currents within power systems [10]-[23]. A simple method reported in [14], [15] locates open-circuit fault transistors by comparing the average of the three phase currents with a threshold. A simple direct current method takes up limited software resources. However, the threshold depends on the load conditions. The current deviation method [16] normalizes the output currents, which reduces the influence of the load conditions. By applying a discrete Fourier transformation to the deviation of the currents, the indicator of the mean value and the fundamental component was used to identify fault conditions and to detect the faulty transistors in around two fundamental periods. An analysis of the current space vector trajectory is very effective in open-circuit fault diagnosis. In [17]-[19], the slope of the current space vector trajectory is used to identify faulty legs and the missing half-cycle of the current waveform is employed to locate faulty switches. The instantaneous frequency of the AC current space vector [17] is zero on the diameter of semicircle when an open-circuit fault occurs. The centroid-based fault detection [20] determines the centroid of a half-cycle of the current waveform. An open-circuit fault is declared if the centroid is not at the origin. These three methods are susceptible to noise under light load or no-load conditions. To overcome this drawback, a normalized DC current method was proposed [21]-[23]. To detect and isolate a faulty transistor, the periodic average of the current was divided by the absolute value of the first harmonic of the ac-currents and then compared with a threshold value. The modified normalized dc current method was proposed [14], [15] for implementation in a closed-loop control scheme. The majority of the above mentioned methods are based on current analysis. They are able to detect IGBT open-circuit faults in over one fundamental period.

The other methods are based on the analysis of the voltages within power systems. Based on the analytical model of a VSI, the method reported in [24]-[28] compared the measured voltages with their reference voltages to detect faulty switches. The analysis was based on the failure introduced errors in the phase voltages in comparison to their normal operational status. The inverter pole voltage, machine phase voltage, system line voltage, and machine neutral voltage were the four criteria used in the diagnosis. The time between a fault occurrence and the diagnosis was half of a fundamental period. In [29], a method was proposed for an improved diagnosis for induction motor drive systems based on an approach that combined the switching pattern and the electric drive line-to-line voltage measurements. However, a more detailed analysis of fault

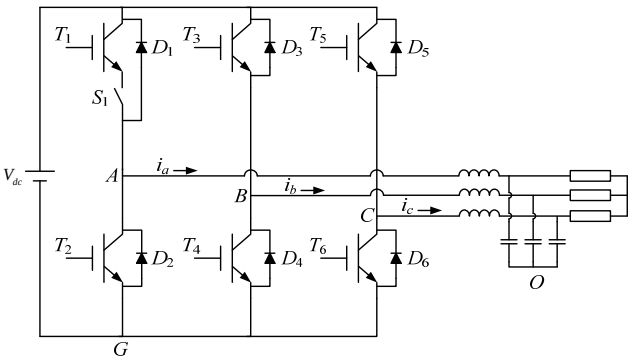

Fig. 1. The common structure of voltage-source inverter.

status and diagnostic time is still needed. An optimized diagnostic voltage was applied to minimize the diagnostic time. The method of sensing voltage across the lower switch [30] was developed basing on the fact that during an open-circuit fault the voltage across the lower switch was around half the bus voltage. Normally, this voltage is either zero or the full bus voltage. With the help of an extra hardware circuit, the diagnostic time is 2.7ms (a fundamental period is 20ms) at the soonest.

This paper presents two diagnostic methods based on the bridge arm pole voltage (method, M1) and the bridge arm line voltage (method, M2). By analyzing the open-circuit faults in voltage-source inverters and with extra simple circuit, these two diagnostic methods are capable of effectively detecting and identifying single and multiple open-circuit faults of inverter IGBTs. The diagnostic time and anti-interference features of these two methods were compared in detail. An experimental study was carried out to show the effectiveness of these two methods and their differences.

The remaining parts of this paper are organized as follows. An analysis of the open-circuit faults in a VSI is shown in Section II. The diagnostic methods of IGBT open-circuit faults are illustrated in Section III. Finally, the experimental results presented in Section IV validate the effectiveness of two diagnosis methods. The summary and some conclusions are given in the final section.

II. Analysis of Open-Circuit Faults in a VSI

The common structure of a VSI is shown in Fig. 1. The power switches were produced by using IGBTs (T_1~T_6) with antiparallel diodes (D_1~D_6). When S_1 is open, T_1 is an open-circuit failure with the antiparallel diode D_1 still conducting. The diagnostic methods employ bridge arm voltages and switching signals based on an analytical model of the VSI. A description of these two methods is given as follows.

(1) Method 1 (M1), bridge arm pole voltage (u_{AG}, u_{BG}, u_{CG}).

(2) Method 2 (M2), bridge arm line voltage (u_{AB}, u_{BC}, u_{CA}).

The bridge arm pole voltage u_{AG} changes after the

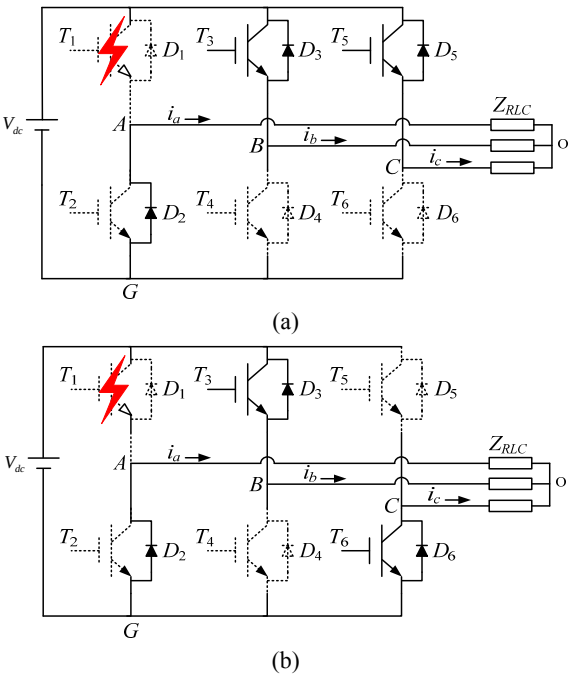

Fig. 2. The status of switches and the current loop when open-circuit fault of T_1 occurs. (a) case i_a>0, i_b>0, T_1=1, T_3=1, T_5=1. (b) case i_a>0, i_b>0, T_1=1, T_3=1, T_5=0.

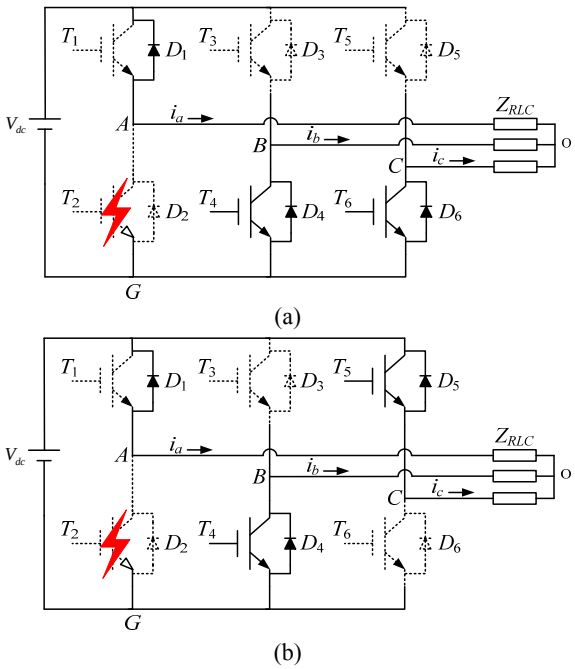

Fig. 3. The status of switches and the current loop when open-circuit fault of T_2 occurs. (a) case i_a<0, i_b<0, T_2=1, T_4=1, T_6=1. (b) case i_a<0, i_b<0, T_2=1, T_4=1, T_6=0.

occurrence of a single or multiple IGBT open-circuit faults. Fig. 2 presents the switches conduction status and the current loop when an open-circuit fault of T_1 occurs. When the phase currents i_a and i_b are positive, and the gate signals T_1 and T_3 are at a high level, and the bridge arm pole voltage u_{AG} is equal to V_{dc} under normal operation conditions. In VSIs with a type Y connected load, the three phase currents have a relationship as shown in Equ. (1).

$$i_a + i_b + i_c = 0 \tag{1}$$

The positive half of the current of phase A is lost when T_1 is associated with an open-circuit failure. Therefore:

$$i_b + i_c = 0 \tag{2}$$

For case (a) (i_a>0, i_b>0, T_1=1, T_3=1, T_5=1) as shown in Fig. 2(a), i_a becomes zero and i_c is negative according to Equ. (2). Then i_c circulates through D_5. Therefore:

$$u_{BO} = u_{CO} = 0 \tag{3}$$

Then the bridge arm pole voltage in case (a) $u_{AG\_case(a)}$ can be expressed as:

$$u_{AG\_case(a)} = u_{OG} = u_{BG} - u_{BO} = V_{dc} \tag{4}$$

For case (b) (i_a>0, i_b>0, T_1=1, T_3=1, T_5=0) as shown in Fig. 2(b), i_c is negative and circulates through T_6. Therefore, the bridge arm pole voltage in case (b) $u_{AG\_case(b)}$ can be written as:

$$u_{AG\_case(b)} = u_{OG} = V_{dc} / 2 \tag{5}$$

Then, the bridge arm pole voltage u_{AG} is be given by:

$$u_{AG} = V_{dc} \,\&\, T_5 + (V_{dc} / 2) \,\&\, \overline{T_5} \tag{6}$$

Where T_5 is the switching signal of the IGBT T_5, and $\overline{T_5}$ is the complementary signal of T_5.

Table I shows the bridge arm pole voltage u_{AG} for a sound inverter and the occurrence of an open-circuit failure of T_1. The case shown as "red" in Table I was analyzed in detail. The cases of the differences between the sound condition of the inverter and an open-circuit failure of T_1 can be examined in the same way. Due to space limitations, the analysis is not presented in this paper. Table I presents the bridge arm pole voltage u_{AG} for a sound inverter and the occurrence of an open-circuit fault of the upper IGBT T_1. There is no difference between these two operating conditions in the negative half cycle of i_a because the current can flow through the antiparallel diode D_1 whether the IGBT T_1 is sound or not. Consequently, the detection of an open-circuit fault of T_1 is feasible only in three cases (labeled as the red and blue cases in Table I).

Fig. 3 presents the status of the switches and current loop when an open-circuit fault of T_2 occurs. Table II shows the bridge arm pole voltage u_{AG} for a sound inverter and when an open-circuit fault of the lower IGBT T_2 occurs. As in the previous situations, an open-circuit fault of T_2 can only be detected in three cases (labeled as the red and blue cases in Table II). These situations correspond to the negative half cycle of the phase current i_a and when the gate signal T_1 is at a high level. During the positive half cycle of the phase current i_a, an open-circuit fault of the lower IGBT cannot be detected.

Tables III-IV give the bridge arm line voltage u_{AB} for a sound inverter and when an open-circuit fault occurs in the upper IGBT T_1 and in the lower IGBT T_2, respectively. Therefore, two types of bridge arm voltages are presented and

TABLE I
BRIDGE ARM POLE VOLTAGE FOR A SOUND INVERTER AND FOR OPEN-CIRCUIT FAILURE OF T_1

i_a	i_b	case	T_1	T_3	sound u_{AG}	open-circuit fault of T_1 u_{AG}
+	+	red	1	1	V_{dc}	$V_{dc}\&T_5+(V_{dc}/2)\&\overline{T_5}$
		blue	1	0	V_{dc}	0
		white	0	1	0	0
		white	0	0	0	0
+	-	white	1	1	V_{dc}	V_{dc}
		blue	1	0	V_{dc}	$(V_{dc}/2)\&T_5$
		white	0	1	0	0
		white	0	0	0	0
-	+	white	*	*	*	same as sound value
-	-	white	*	*	*	same as sound value

* in table indicates all possible states.

TABLE II
BRIDGE ARM POLE VOLTAGE FOR A SOUND INVERTER AND FOR OPEN-CIRCUIT FAILURE OF T_2

i_a	i_b	case	T_2	T_4	sound u_{AG}	open-circuit fault of T_4 u_{AG}
-	-	red	1	1	0	$(V_{dc}/2)\&\overline{T_6}$
		blue	1	0	0	V_{dc}
		white	0	1	V_{dc}	V_{dc}
		white	0	0	V_{dc}	V_{dc}
-	+	white	1	1	0	0
		blue	1	0	0	$V_{dc}\&\overline{T_6}+(V_{dc}/2)\&T_6$
		white	0	1	V_{dc}	V_{dc}
		white	0	0	V_{dc}	V_{dc}
+	+	white	*	*	*	same as sound value
+	-	white	*	*	*	same as sound value

* in table indicates all possible states.

TABLE III
BRIDGE ARM LINE VOLTAGE FOR A SOUND INVERTER AND FOR OPEN-CIRCUIT FAILURE OF T_1

i_a	i_b	case	T_1	T_3	sound u_{AB}	open-circuit fault of T_1 u_{AB}
+	+	red	1	1	0	$-(V_{dc}/2)\&\overline{T_5}$
		blue	1	0	V_{dc}	0
		white	0	1	$-V_{dc}$	$-V_{dc}$
		white	0	0	0	0
+	-	white	1	1	0	0
		blue	1	0	V_{dc}	$(V_{dc}/2)\&T_5$
		white	0	1	×	×
		white	0	0	0	0
-	+	white	*	*	*	same as sound value
-	-	white	*	*	*	same as sound value

* in table indicates all possible states, × indicates nonexistent states.

TABLE IV
BRIDGE ARM LINE VOLTAGE FOR A SOUND INVERTER AND FOR OPEN-CIRCUIT FAILURE OF T_2

i_a	i_b	case	T_2	T_4	sound u_{AB}	open-circuit fault of T_4 u_{AB}
-	-	red	1	1	0	$(V_{dc}/2)\&\overline{T_6}$
		blue	1	0	$-V_{dc}$	0
		white	0	1	V_{dc}	V_{dc}
		white	0	0	0	0
-	+	white	1	1	0	0
		blue	1	0	$-V_{dc}$	$-(V_{dc}/2)\&T_6$
		white	0	1	×	×
		white	0	0	0	0
+	+	white	*	*	*	same as sound value
+	-	white	*	*	*	same as sound value

* in table indicates all possible states, × indicates nonexistent states.

analyzed to establish the differences between the normal operating conditions and the open-circuit faulty conditions.

III. DIAGNOSTIC METHODS OF IGBTS OPEN-CIRCUIT FAULTS

The above analysis shows that the information obtained on faults is based on the switching signals and the measured bridge arm voltage. To distinguish the bridge arm voltage under faulty conditions from the normal voltage, an extra simple hardware circuit, shown in Fig. 4, is implemented. M1 is extracted from Table I-II based on the blue and red cases collectively for the open-circuit faults. There is no difference between the normal and faulty conditions in the white cases.

The value of u_{ref1} is chosen between $V_{dc}/2$ and V_{dc} (relative to u_{AG}) for the colored cases (red and blue cases) in Table I. Therefore, the output signal V_{J1} of the Not gate varies from the low level to the high level. On combining the switching signal T_1, the open-circuit fault of T_1 is given by the Boolean signal as shown in Equ. (7).

$$F_{T_1\_M1} = T_1 \,\&\, V_{J1} \tag{7}$$

Where $F_{T_1\_M1}$ is the indicator signal for an open-circuit fault of T_1 by M1.

For the detection of the lower IGBT T_2, the value of u_{ref2} is chosen between $-V_{dc}$ and $-V_{dc}/2$ (relative to u_{AG}) for the colored cases (red and blue cases) in Table II. Therefore, the output signal V_{J2} of the comparator (COMP 2) varies from the low level to the high level. On combining the switching signal T_2, the open-circuit fault of T_2 is given by the Boolean signal as shown in Equ. (8).

$$F_{T_2\_M1} = T_2 \,\&\, V_{J2} \tag{8}$$

The blue and red cases are different in the fault diagnosis for M2, and these are given in Table III-IV. Therefore, the Boolean signals could easily be obtained as shown by Equs. (9)-(10).

$$F_{T_1\_M2} = T_1 \,\&\, T_4 \,\&\, V_{J1} \tag{9}$$

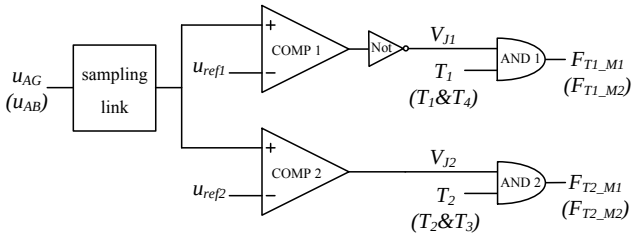

Fig. 4. The additional simple hardware circuit implemented in the proposed diagnostic methods.

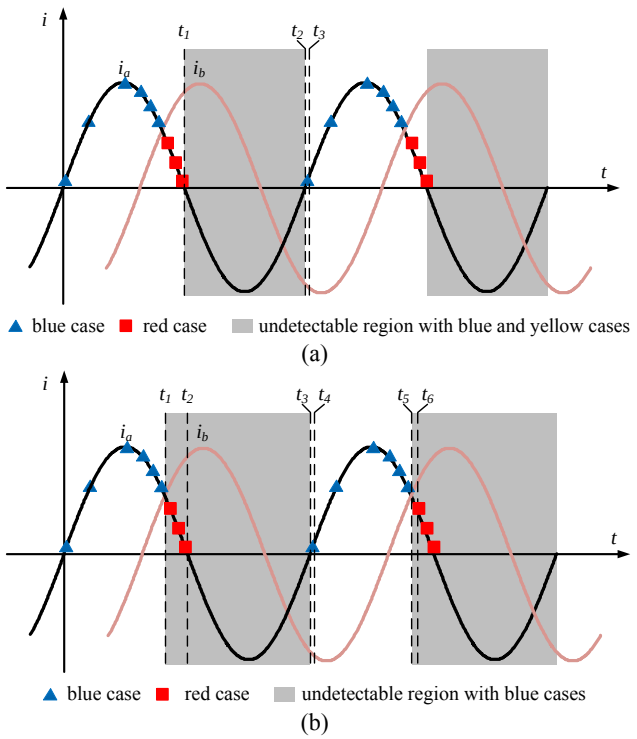

Fig. 5. The diagnostic intervals of T_1 and phase currents i_a and i_b (the switching frequency is shown three times the fundamental frequency for easy understanding). (a) M1. (b) M2.

$$F_{T_2\_M2} = T_2 \,\&\, T_3 \,\&\, V_{J2} \tag{10}$$

Where $F_{T_1\_M2}$ is the indicator signal for an open-circuit fault of T_1 by M2.

A. Detecting Time

The colored cases shown in Table I-IV are depicted intuitively in Fig. 5. For ease of understanding the switching frequency in this figure is shown as three times the fundamental frequency. The dots shown with colors on the phase currents are the diagnostic intervals. For example, the red dots correspond to the red cases in the Tables. Combining T_1 (T_1 and T_4), the switching signal and the bridge arm voltage u_{AG} (u_{AB}), an open-circuit fault of T_1 can be detected. It is worth noting that both of the red cases with T_1 and T_3 occur when current i_b is more than i_a.

If a failure of T_1 occurs at any instant of time between t_2 and t_5, using the red case M2 detects it at time, t_6, as shown in Fig. 5(b). Therefore, the diagnostic time of this method is 11/12 of the fundamental period in the worst case. However, it can be reduced to 7/12 of the fundamental period by using the blue cases. The red and blue cases, which can be obtained from Table I-II, can be used together in M1. Then, M1 using red and blue cases is able to detect the failure at time t_3 if an open-circuit fault of T_1 occurs at any instant of time between t_1 and t_2, as shown in Fig. 5(a).

Therefore, the diagnostic time of M1 is smaller than that of M2 and it is half of the fundamental period in the worst case.

B. Resistivity Against False Alarms

The proposed method is based on the bridge arm voltage instead of the phase currents which are sensitive to noise. As a result, false alarms hardly ever occur during light-loads and under transient conditions. However, under real operating conditions, false alarms can trigger at the time of the turning-on and turning-off processes of IGBTs [29] and the delay time is in consistence with the characteristic features of IGBTs which has been studied in detail [31]. Thus, the modified switching signals have been implemented. The switching signal of T_1 can be modified as shown in Equ. (11).

$$T_1^{'} = T_{1\_delay} \,\&\, T_1 \tag{11}$$

Where T_{1_delay} is the delay time, and $T_1^{'}$ is the modified switching signal of T_1.

Therefore, Equs. (7)-(10) can be modified as:

$$F_{T_1\_M1} = T_1^{'} \,\&\, V_{J1} \tag{12}$$

$$F_{T_2\_M1} = T_2^{'} \,\&\, V_{J2} \tag{13}$$

$$F_{T_1\_M2} = T_1^{'} \,\&\, T_4^{'} \,\&\, V_{J1} \tag{14}$$

$$F_{T_2\_M2} = T_2^{'} \,\&\, T_3^{'} \,\&\, V_{J2} \tag{15}$$

Thus, the proposed methods are effective and can successfully indicate faulty IGBTs. This statement is validated in the next section.

IV. Experimental Results

In order to confirm the feasibility of the fault diagnostic methods, experiments were conducted under the specifications presented in Table V. A 1kW rated power three-phase voltage-source inverter was built (Fig. 6), using Infineon IGBTs (IKW40T120) in TrenchStop and Fieldstop technology with a soft fast recovery anti-parallel emitter controlled HE diode.

Fig. 7 shows experimental results of the three phase currents and alarm signal obtained when an open-circuit fault of the upper IGBT T_1 occurs in the detectable region of the positive cycle of i_a. Under normal operating conditions, the three phase currents are sinusoidal and the alarm signal F_{T1} (F_{T1_M1} or F_{T1_M2}) is equal to zero. When a failure takes place at the instant FO_1 (fault occurrence), i_a drops sharply to zero and the alarm signal F_{T1} detects the failure within 280ns, since the fault occurs in the diagnostic range (blue case) revealed in Fig. 5.

TABLE V
SPECIFICATIONS OF THE VSI

DC-link Voltage	400 V
Phase Voltage	110 V_{rms} 50 Hz
Rated Power	1000 W
Switching Frequency	10 kHz
Dead Time	2 μs
IGBT	IKW40T120

TABLE VI
PROPAGATION DELAY TIME OF EXTRA HARDWARE CIRCUIT

Sampling	LMH6611	<100n
Comparing	TLV3202	<50ns
NOT link	CD74AC00	<10ns
AND link	CD74AC08, SN74AC11	<10ns

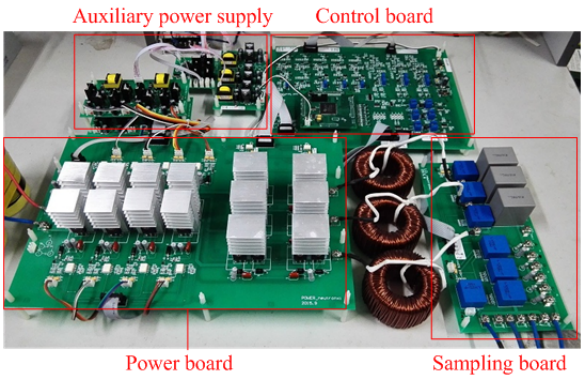

Fig. 6. Experimental setup.

The diagnostic time is a summation of the delays in the propagation time from the extra hardware circuit, which is comprised of two sampling links, one comparing link, one NOT link and two AND links. As presented in Table VI, the diagnostic times of M1 and M2 take place within 280ns at the soonest.

At the same time, the digital signal processor (DSP) captures the faulty signal and takes steps to prevent secondary failures. If a failure is introduced at the instant FO2 in Fig. 7 (undetectable region), the failure cannot be detected until ia reaches zero in value. Therefore the diagnostic times of M1 and M2 are not more than 1/2 (10ms) and 7/12 (11.67ms) of the fundamental period, respectively. Fig. 8 also confirms this conclusion.

Figs. 9-10 show experimental results of the three phase currents and the alarm signal when an open-circuit fault of the lower IGBT T_2 occurs in the detectable and undetectable regions, respectively. By examining these figures the same conclusions previously mentioned are reached. When a failure is allowed to occur at the instant FO_1 (fault occurrence) as shown in Fig. 9, the alarm signal F_{T2} detects the failure within 280ns. If a failure is allowed at the instant FO_2 (undetectable region), the diagnostic times of M1 and M2 are

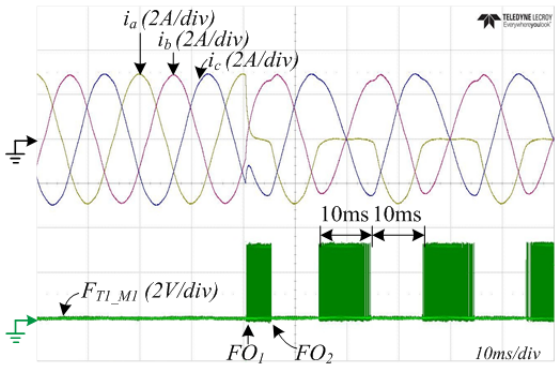

(a)

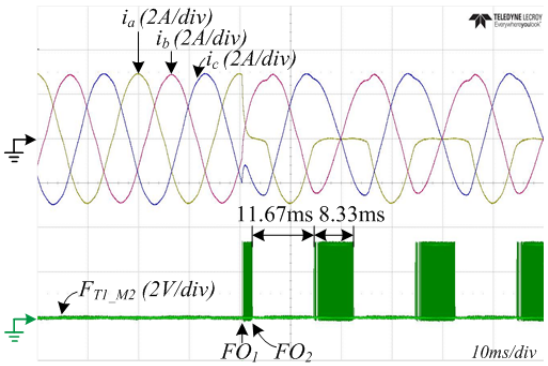

(b)

Fig. 7. Experimental results of phase currents and alarm signal for open-circuit fault of T_1 occurring in the detectable region. (a) M1. (b) M2.

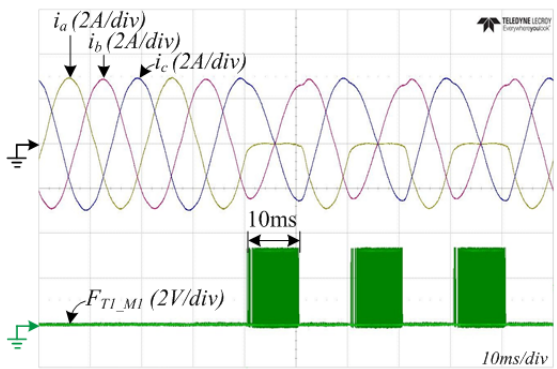

(a)

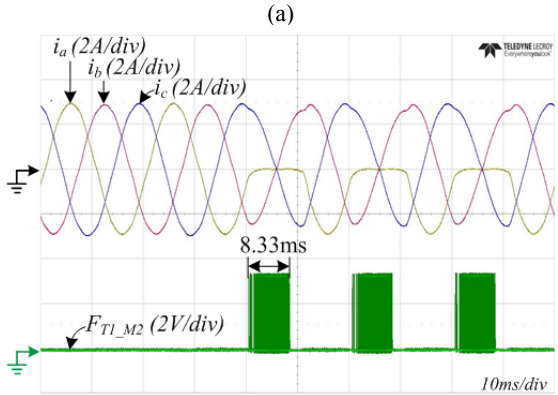

(b)

Fig. 8. Experimental results of phase currents and alarm signal for open-circuit fault of T_1 occurring in the undetectable region. (a) M1. (b) M2.

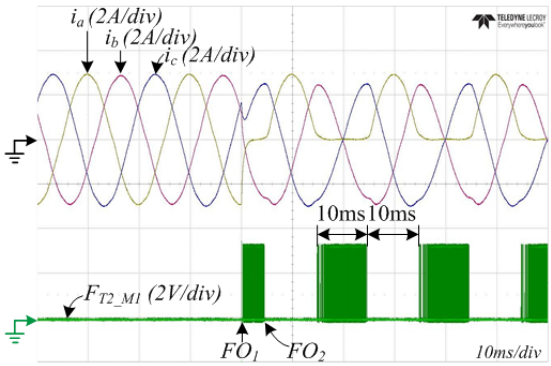

(a)

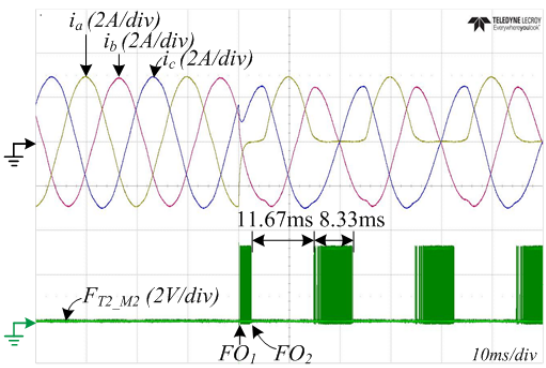

(b)

Fig. 9. Experimental results of phase currents and alarm signal for open-circuit fault of T_2 occurring in the detectable region. (a) M1. (b) M2.

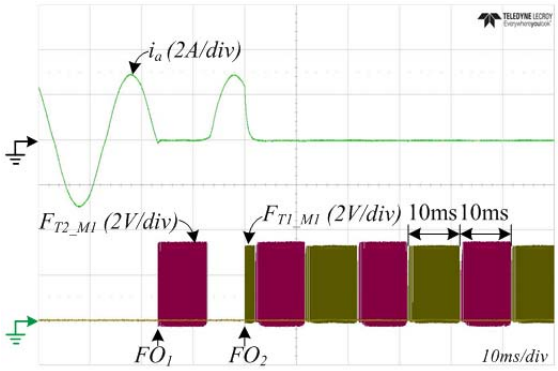

(a)

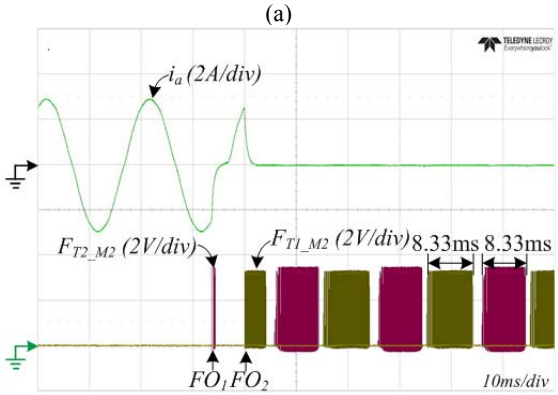

(b)

Fig. 11. Experimental results of phase current i_a and alarm signals F_{T1} and F_{T2}, for open-circuit fault of T_1 and T_2 occurring simultaneously. (a) M1. (b) M2.

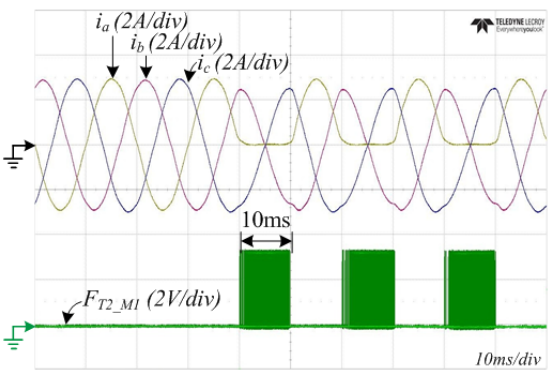

(a)

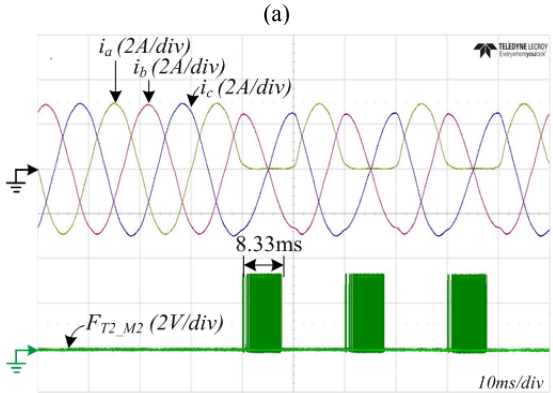

(b)

Fig. 10. Experimental results of phase currents and alarm signal for open-circuit fault of T_2 occurring in the undetectable region. (a) M1. (b) M2.

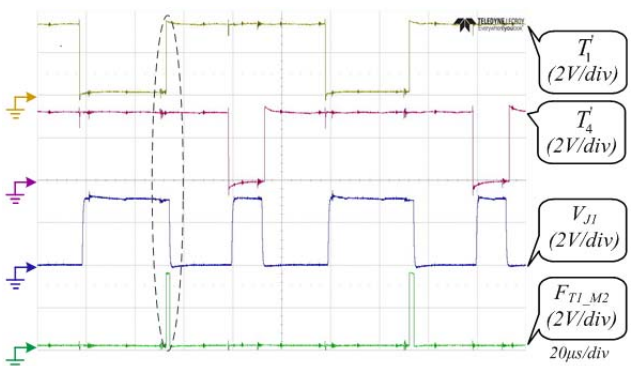

(a)

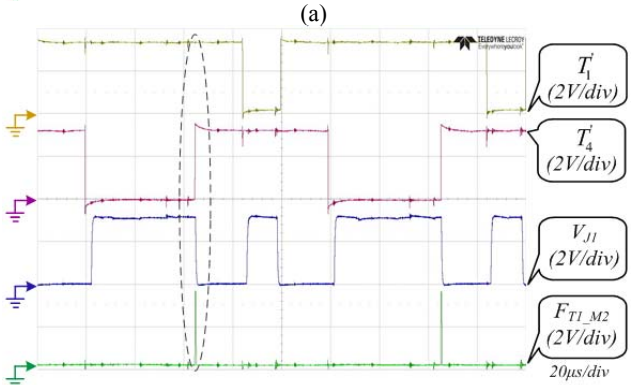

(b)

Fig. 12. Experimental results of diagnostic logic signals and alarm signal F_{T1_M2}. (a) false alarm occurring at time T_1 turning on. (b) false alarm occurring at time T_4 turning on.

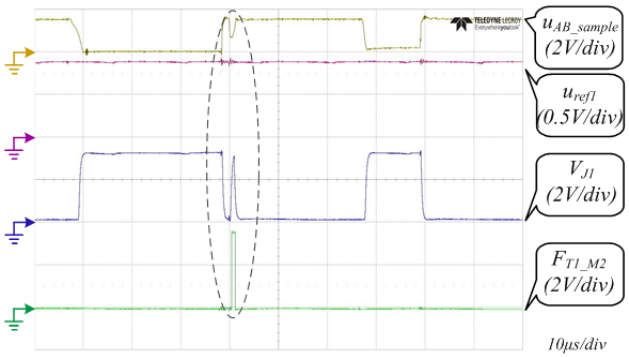

(a)

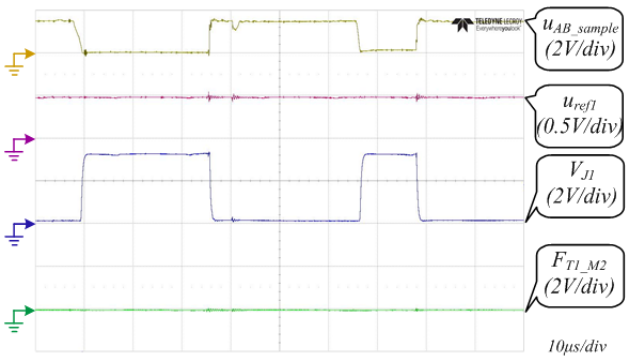

(b)

Fig. 13. Experimental results of u_{AB}, u_{ref1}, V_{J1} and F_{T1_M2}. (a) u_{ref1}=0.88V. (b) u_{ref1}=0.49V.

not more than 1/2 (10ms) and 7/12 (11.67ms) of the fundamental period, respectively.

Fig. 11 shows experimental results obtained for the phase current i_a, alarm signals F_{T1} and F_{T2} when an open-circuit fault of the lower IGBT T_2 occurs at the instant FO_1 and when an open-circuit fault of the upper IGBT T_1 occurs at the instant FO_2. The alarm signals F_{T2} (F_{T2_M1} or F_{T2_M2}) and F_{T1} (F_{T1_M1} or F_{T1_M2}) interact within 280ns. Therefore, both M1 and M2 are effective in detecting one phase IGBT open-circuit faults.

False alarms appear at the time instants when T_1 and T_4 turn on as shown in Fig. 12(a) and Fig. 12(b), respectively. Therefore, the diagnostic logic of the proposed methods were modified according to Equs. (12)-(15) with an adjustable delay time of 0-5μs, which is effective against the false alarms caused by the IGBT switching process. Fig. 13(a) shows the false alarm signal F_{T1_M2} caused by voltage interference on u_{AB_sample} (sampling voltage of u_{AB}), which is smaller than the comparison voltage (u_{ref1} of 0.88V)). Obviously, the false alarms vanish when the comparison voltage is 0.49V as shown in Fig. 13(b). As a matter of fact, the comparison voltage can be set over a wide range under actual operating conditions. These conclusions are similar to those reached with M1. Therefore, these two diagnostic methods are robust against interference and noise with a small comparison voltage.

V. CONCLUSIONS

Two diagnostic methods for open-circuit fault diagnosis in voltage source inverter systems were proposed and their performances were discussed. One method was based on the bridge arm pole voltage, and the other was based on the bridge arm line voltage. With the addition of an extra simple circuit, these two diagnostic methods detected and identified single and multiple open-circuit faults of inverter IGBTs effectively and rapidly. These methods were based on an analytical model of a VSI. The diagnostic time of the two methods was less than 280ns in the best case. The diagnostic time of the method, M1 was smaller than that of the method, M2 and was half of the fundamental period in the worst case. Both of these methods were found to be robust and unsusceptible to strong load transients and noise interference. In addition, the diagnostic logic was only related to the switch status, which makes these two methods practical under different load conditions. An experimental study was carried out to demonstrate the effectiveness of these two methods and also their differences. The method M1 possessed superior features. With the addition of an extra simple analog circuit, M1 was found suitable for application to VSI systems. Both of the methods can effectively handle all types of open-circuit faults. They can also shut down a system or turn it on to run in the backup operation mode, and avoid secondary failures caused by open-circuit faults.

ACKNOWLEDGMENT

This project supported by the State Key Program of National Natural Science of China (Grant No. 51337009).

REFERENCES

[1] C. Brunson, L. Empringham, L. de Lillo, P. Wheeler, and J. Clare, "Open-circuit fault detection and diagnosis in matrix converters," *IEEE Trans. Power Electron.*, Vol. 30, No. 5, pp. 2840-2847, May 2015.

[2] U.-M. Choi, F. Blaabjerg, and K.-B. Lee, "Study and handling methods of power IGBT module failures in power electronic converter systems," *IEEE Trans. Power Electron.*, Vol. 30, No. 5, pp. 2517-2533, May 2015.

[3] S. Yang, A. Bryant, P. Mawby, D. Xiang, L. Ran, and P. Tavner, "An industry-based survey of reliability in power electronic converters," *IEEE Trans. Ind. Appl.*, Vol. 47, No. 3, pp. 1441-1451, May/Jun. 2011.

[4] K. Abdennadher, P. Venet, G. Rojat, J.-M. Retif, and C. Rosset, "A real-time predictive-maintenance system of aluminum electrolytic capacitors used in uninterrupted power supplies," *IEEE Trans. Ind. Appl.*, Vol. 46, No. 4, pp. 1644-1652, Jul./Aug. 2010.

[5] T. H. Nguyen, Q. A. Le, and D.-C. Lee, "Estimation of ESR in the DC-link capacitors of AC motor drive systems with a front-end diode rectifier," *Journal of Power Electronics*, Vol. 15, No. 2, pp. 411-418, Mar. 2015.

[6] H. Sheng, F. Wang, and C. W. Tipton, "A fault detection and protection scheme for three-level DC–DC converters

based on monitoring flying capacitor voltage," *IEEE Trans. Power Electron.*, Vol. 27, No. 2, pp. 685-697, Feb. 2012.
[7] K. S. Smith, L. Ran, and J. Penman, "Real-time detection of intermittent misfiring in a voltage-fed PWM inverter induction-motor drive," *IEEE Trans. Ind. Electron.*, Vol. 44, No. 4, pp. 468-476, Aug. 1997.
[8] F. W. Fuchs, "Some diagnosis methods for voltage source inverters in variable speed drives with induction machines - a survey," in *Proc. IECON*, pp. 1378-1385, 2003.
[9] B. Lu and S. K. Sharma, "A literature review of IGBT fault diagnostic and protection methods for power inverters," *IEEE Trans. Ind. Appl.*, Vol. 45, No. 5, pp. 1770-1777, Sep./Oct. 2009.
[10] N.-H. Kim, W.-S. Baik, M.-H. Kim, and C.-H. Choi, "Rotor fault detection system for the inverter driven induction motor using current signals," *Journal of Power Electronics*, Vol. 9, No. 2, pp. 271-277, Mar. 2009.
[11] S. Khomfoi, W. Sae-Kok, and I. Ngamroo, "An open circuit fault diagnostic technique in IGBTs for AC to DC converters applied in microgrid applications," *Journal of Power Electronics,* Vol. 11, No. 6, pp. 801-810, Nov. 2011.
[12] M. Shahbazi, P. Poure, S. Saadate, and M. R. Zolghadri, "FPGA-based fast detection with reduced sensor count for a fault-tolerant three-phase converter," *IEEE Trans. Ind. Informat.*, Vol. 9, No. 3, pp. 1343-1350, Aug. 2013.
[13] B.-G. Park, K.-J. Lee, R.-Y. Kim, and D.-S. Hyun, "Low-cost fault diagnosis algorithm for switch open-damage in BLDC motor drives," *Journal of Power Electronics,* Vol. 10, No. 6, pp. 702-708, Nov. 2010.
[14] K. Rothenhagen and F. W. Fuchs, "Performance of diagnosis methods for IGBT open circuit faults in voltage source active rectifiers," in *Proc PESC*, pp. 4348-4354, 2004.
[15] K. Rothenhagen and F. W. Fuchs, "Performance of diagnosis methods for IGBT open circuit faults in three phase voltage source inverters for AC variable speed drives," in *Proc EPE*, pp. 1-10, 2005.
[16] C. Kral and K. Kafka, "Power electronics monitoring for a controlled voltage source inverter drive with induction machines," in *Proc P*ESC, pp. 213-217, 2000.
[17] R. Peuget, S. Courtine, and J. P. Rognon, "Fault detection and isolation on a PWM inverter by knowledge-based model," *IEEE Trans. Ind. Appl.*, Vol. 34, No. 6, pp. 1318-1326, Nov./Dec. 1998.
[18] H.-S. Ro, D.-H. Kim, H.-G. Jeong, and K.-B. Lee, "Fault tolerant control for power transistor faults in switched reluctance motor drives," *IEEE Trans. Ind. Appl.*, Vol. 51, No. 4, pp. 3187-3197, Jul./Aug. 2015.
[19] J. F. Martins, V. F., Pires, C. Lima, and A. J. Pires, "Fault detection and diagnosis of grid-connected power inverters using PCA and current mean value," in *Proc IECON*, pp. 5185-5190, 2012.
[20] P. Gilreath and B. N. Singh, "A new centroid based fault detection method for 3-phase inverter-fed induction motors," in *Proc PESC*, pp. 2664-2669, 2005.
[21] S. Abramik, W. Sleszynski, J. Niezaniski, and H. Piquet, "A diagnostic method for on-line fault detection and localization in VSI-fed AC drives," in *Proc EPE*, pp. 1-8, 2003.
[22] J. F. Marques, J. O. Estima, N. S. Gameiro, and A. J. M. Cardoso, "A new diagnostic technique for real-time diagnosis of power converter faults in switched reluctance motor drives," *IEEE Trans. Ind. Appl.*, Vol. 50, No. 3, pp. 1854-1860, May/Jun. 2014.
[23] C. Choi and W. Lee, "Design and evaluation of voltage measurement-based sectoral diagnosis method for inverter open switch faults of permanent magnet synchronous motor drives," *IET Power Appl.*, Vol. 6, No. 8, pp. 526-532, Sep. 2012.
[24] R. L. A. Ribeiro, C. B. Jacobina, E. R. C. da Silva, and A. M. N. Lima, "Fault detection in voltage-fed PWM motor drive systems," in *Proc PESC*, pp. 242-247, 2000.
[25] R. L. de Araujo Ribeiro, C. B. Jacobina, E. R. C. da Silva, and A. M. N. Lima, "Fault detection of open-switch damage in voltage-fed PWM motor drive systems," *IEEE Trans. Power Electron.*, Vol. 18, No. 2, pp. 587-593, Mar. 2003.
[26] M. Trabelsi, M. Boussak, P. Mestre, and M. Gossa, "Pole voltage based-approach for IGBTs open-circuit fault detection and diagnosis in PWM-VSI-Fed induction motor drives," in *Proc POWERENG*, pp. 1-6, 2011.
[27] S.-M. Jung, J.-S. Park, H.-W. Kim, K.-Y. Cho, and M.-J. Youn, "An MRAS-based diagnosis of open-circuit fault in PWM voltage-source inverters for PM synchronous motor drive systems," *IEEE Trans. Power Electron.*, Vol. 28, No. 5, pp. 2514-2526, May 2013.
[28] B.-G. Park, R.-Y. Kim, and D.-S. Hyun, "Open circuit fault diagnosis using stator resistance variation for permanent magnet synchronous motor drives," *Journal of Power Electronics*, Vol. 13, No. 6, pp. 985-990, Nov. 2013.
[29] M. Trabelsi, M. Boussak, P. Mestre, and M. Gossa, "An improved diagnosis technique for IGBTs open-circuit fault in PWM-VSI-fed induction motor drive," in *Proc IEEE ISIE*, pp. 2111-2117, 2011.
[30] O.-S. Yu, N.-J. Park, and D.-S. Hyun, "A novel fault detection scheme for voltage fed PWM inverter," in *Proc IECON*, pp. 2654-2659, 2006.
[31] Q.-T. An, L.-Z. Sun, K. Zhao, and L. Sun, "Switching function model based fast-diagnostic method of open-switch faults in inverters without sensors," *IEEE Trans. Power Electron.*, Vol. 26, No. 1, pp. 119-126, Jan. 2011.

Yuxi Wang was born in Zhejiang, China, in 1988. He received his B.S. degree in Electrical Engineering from Zhejiang University, Hangzhou, China, in 2011; where he is presently working towards his Ph.D. degree. His current research interests include dc/dc converters and the fault diagnosis of power electronic circuits and systems.

Zhan Li was born in Hunan, China, in 1992. He received his B.S. degree in Electrical Engineering from Zhejiang University, Hangzhou, China, in 2014; where he is presently working towards his Ph.D. degree. His current research interests include LED drives and the fault diagnosis of power electronic circuits and systems.

Minghui Xu was born in Shandong, China, in 1991. He received his B.S. degree in Electrical Engineering from Zhejiang University, Hangzhou, China, in 2014; where he is presently working towards his M.S. degree. His current research interests include high power dc/dc converters.

Hao Ma was born in Hangzhou, China, in 1969. He received his B.S., M.S. and Ph.D. degrees in Electrical Engineering from Zhejiang University, Hangzhou, China, in 1991, 1994 and 1997, respectively. He is presently working as a Professor in the College of Electrical Engineering, Zhejiang University. From September 2007 to September 2008, he was a Delta Visiting Scholar at North Carolina State University, Raleigh, NC, USA. His current research interests include advanced control in power electronics, fault diagnosis of power electronic circuits and systems, and the application of power electronics.